Electrochemical Separation of Ag_2S and Cu_2S from Molten Sulfide Electrolyte

Mary-Elizabeth Wagner, Antoine Allanore

Department of Materials Science and Engineering, Massachusetts Institute of Technology, Cambridge, United States of America

Abstract. The production of precious metals from Cu-rich sources such as ore products or secondary sources is slow and complex largely due to limited solubility in aqueous electrolytes. This results in sequential processing with various electrolytes and chemistries, where first Cu is electrorefined, followed by Ag, followed by Au and the platinum group metals. These are separate processes, often conducted in separate electrorefining and electrowinning facilities. The chemical properties of molten sulfides, and their ability to operate at a temperature where liquid metal cathodes are used, suggest the possibility of an alternative, streamlined processing route for Cu and precious metals. Unfortunately, little thermodynamic or electrochemical information is available regarding the behavior of Cu and precious metal sulfides in molten sulfide electrolytes. Herein, the *relative* activity of the Cu_2S-Ag_2S pseudobinary dissolved in a BaS-La_2S_3 supporting electrolyte is measured at 1523 K. It was found that the supporting electrolyte favors mixing with Ag_2S over Cu_2S. Molten sulfide electrolysis of Cu and Ag was conducted, with results in good agreement with the thermodynamic model. It is found that the Ag-Cu cathode chemistry will influence the electrochemical selectivity in the Ag-Cu-Ba-La-S system.

Keywords: precious metal extraction; molten sulfide electrolysis; e-waste recycling;

1. Introduction

The solubility limitations of aqueous electrolytes pose a challenge for sustainable processing of precious metals (such as Ag, Au and platinum group metals) from Cu-rich sources. Traditionally, these high value metals must first go through the Cu pipeline until they are recovered as by-products during electrorefining. Ag and other high value metals are insoluble in the $CuSO_4$-based electrolyte, and collect at the bottom of the Cu refining cells as slimes. The refining cells must be cleaned periodically to collect these slimes, which primarily take the form of selenides (which contain the precious metals) and sulfates (containing base metals, elements such as lead and arsenic, as well as some residual copper) [1, 2, 3, 4, 5, 6]. There are many differing techniques for treating slimes, extensively discussed in literature [1, 7, 8, 9]. These methods often utilize a combination of pyro- and hydro- metallurgical techniques to successfully produce a metallic phase ready for further electrorefining, and are generally optimized for the typical slime composition at each refinery. However, in all cases, this process can only be done in series, using multiple facilities and separate streams for each metal, beginning with Cu, followed by Ag, then Au, then the platinum group metals. As a result, platinum group metals recovered from Cu ores are tied to the processes of at least three different metals (Cu, Ag, and Au), and thus must undergo slime treatment at least three times.

The challenges with extracting precious metals from Cu-rich sources exist regardless of the initial material's status as a primary ore or a secondary recycled waste, because the process streams are merged at the smelter and a Cu anode with mixed primary and recycled origins undergoes electrorefining. These Cu anodes can contain valuable metals such as Ag, Au, Pd, and Pt. 10.5 wt% Ag and 1.8 wt% Au were reported in slimes at Sumitomo Metal Mining Co. Ltd. [10], and some slimes can contain up to 50wt% Cu due to dendrite break-off [1], highlighting some of the inefficiencies of this process.

Higher temperature, non-aqueous electrolytes operating with liquid cathodes should not produce such slimes, and there can be no dendrite break-off from a liquid cathode pool at the bottom of a high temperature refining cell, which is the most common design for such cells. Molten sulfides have already shown promise as a stable high temperature electrolyte with sufficient ionic conductivity to support electrolysis. They have been a successful media for electrolytic decomposition of the sulfides of copper, molybdenum, and rhenium [11, 12]. Furthermore, Cu, Au, Ag, Pt, and Pd have all been found in nature as sulfides [13, 14, 15, 16], supporting the likelihood that they could all be solvated in a molten sulfide electrolyte. It is the present lack of an available solvent capable of dissolving multiple precious elements together that necessitates their sequential processing and increased environmental burden [1, 2, 7, 8, 10, 9, 17]. Preliminary tests of precious metal solubility in molten sulfides have been reported in [18].

In order to investigate molten sulfides as possible electrolytes for extracting precious metals from Cu-rich sources, an electrowinning study of the behavior of Cu and Ag sulfides was carried out. On the electrochemical series plotted for several sulfides in Figure 1, the standard state decomposition potentials of Cu from Cu_2S and Ag from Ag_2S are 0.257 V apart, greater than the 0.2 V threshold commonly used to assess electrochemical separation feasibility [19, 20]. However, this metric assumes that all species are behaving as if they were pure, or at their stoichiometric composition (i.e. in their standard state), which is not a realistic assumption for true electrolysis, wherein the electroactive species are dissolved in a supporting electrolyte. In reality, the supporting electrolyte will chemically interact with the electroactive species, shifting their thermodynamic activities and, as a result, their decomposition potentials. If an alloy cathode is used instead of a pure cathode, the metallic species will also deviate from standard state. Recent work in studying electrochemical separation has shown that equilibrium electrochemical synthesis diagrams (EESD) are a more accurate metric to predict the electrolyzed product. EESD's link the equilibrium composition of the alloy deposited at the cathode to the real (non-standard state) decomposition potential difference of electrolyte species [21, 22]. This allows for the electrochemist to model co-deposition of two competing species in the reduction reaction.

In the case of Ag-Cu, the equilibrium electrochemical synthesis diagram predicts considerable drive for alloying at 1523K. Starting with the standard state decomposition potential difference of 0.257 V, Figure 2 predicts 0.062 molar fraction Cu to deposit on an Ag cathode, suggesting that the energetics of mixing Ag and Cu metal will play a signifiant role in electrodeposition. However, liquid sulfides have been shown previously to exhibit behavior that depart from standard state or ideal behavior [23, 24]. Therefore, the assumption that the actual decomposition potential difference in a supporting electrolyte remains at 0.257 V is likely invalid. In order to understand the true thermodynamic nature of the electrolyte, it is necessary to measure the activities of Cu_2S and Ag_2S in a molten sulfide supporting electrolyte. An electrolyte consisting of BaS-La_2S_3 has previously shown to be a good candidate for supporting stable and successful electrolysis of Cu from Cu_2S [12]. Therefore, BaS-La_2S_3 was chosen as the supporting electrolyte for the Cu_2S-Ag_2S system.

The ability of molten sulfides to solubilize many different materials make traditional electrochemical activity measurements challenging. Metal references are contaminated by exchange interactions and metallothermic reduction, which cause the reference to gradually change composition over the course of the experiment, creating a shift in electrochemical measurements. Attempts to use an ion-selective β''-Al_2O_3 membrane were unsuccessful due to exchange interactions between aluminum and barium. The possibility of making a reference electrode inspired by aqueous capillary reference electrodes was explored, but again unsuccessful due to electrolyte reaction with the chosen refractory materials (alumina tubes and alumina paste). Because of this, an approach using *relative* activity measurements was used instead. In a relative activity measurement, an EESD is used to measure the decomposition potential difference of two electrolyte species, in this case E_{Ag} and E_{Cu}. This potential difference can be linked to the activities a_{Ag_2S} and a_{Cu_2S} with the equation:

$$E_{\mathrm{Ag}} - E_{\mathrm{Cu}} = E^{\circ}_{\mathrm{Ag}} - \frac{RT}{n_{\mathrm{Ag}}F} \ln a_{\mathrm{Ag_2S}} - (E^{\circ}_{\mathrm{Cu}} - \frac{RT}{n_{\mathrm{Cu}}F} \ln a_{\mathrm{Cu_2S}}) \tag{1}$$

The standard state electrochemical potentials E°_{Ag} and E°_{Cu} are known, and the actual difference in potential $E_{\mathrm{Ag}} - E_{\mathrm{Cu}}$ can be measured by plotting the cathode composition after equilibration on an EESD. The original derivation of this equation, given for a binary ideal solution, can be found in [21]. A re-derivation and expansion of this equation in order to apply to generalized solutions outside their standard state is not shown here, but is given by the authors in [22]. The entire equation may then be solved for a ratio of the activities:

$$\frac{a_{\mathrm{Ag_2S}}}{a_{\mathrm{Cu_2S}}} \tag{2}$$

Although the activities of $\mathrm{Ag_2S}$ and $\mathrm{Cu_2S}$ cannot be measured independently, a relative reference state can still probe the thermodynamic behavior of $\mathrm{Ag_2S}$ and $\mathrm{Cu_2S}$ in the supporting electrolyte. The ratios of two activities in a solution remain constant regardless of which thermodynamic reference state is used [25]. Therefore a relative reference state such as the Wagner-Allanore reference state can be linked to a traditional Raoultian reference state by[18]:

$$\frac{a_B^{WA}}{a_A^{WA}} = \frac{a_B^{R}}{a_A^{R}} \tag{3}$$

The Wagner-Allanore reference state is given by:

$$a_i^{WA} = \rho_i \chi_i \tag{4}$$

Where ρ_i is the Wagner-Allanore activity coefficient of i, and χ_i is the relative composition of i along a pseudobinary. ρ of the more electropositive species is set to unity, such that ρ_{Ag_2S}=1 and $a^{WA}_{Cu_2S}$ is measured relative to $a^{WA}_{Ag_2S}$. When activity is framed this way, the relative activity coefficient ρ_{Cu_2S} is in fact the ratio of the Raoultian activity coefficients γ_{Cu_2S} and γ_{Ag_2S}:

$$\rho_{Cu_2S} = \frac{\gamma_{Cu2S}}{\gamma_{Ag_2S}} \tag{5}$$

This framework is useful for understanding if the system will favor codeposition, reducing both elements, or purification, leaving one element in the electrolyte. Although the activities of the supporting BaS-$\mathrm{La_2S_3}$ electrolyte are not measured, their effect on the thermodynamics of $\mathrm{Ag_2S}$ and $\mathrm{Cu_2S}$ are captured in ρ_{Cu_2S}. For example, if the supporting electrolyte favors mixing with $\mathrm{Ag_2S}$ ($\gamma_{Ag_2S} < 1$), while phase separating with $\mathrm{Cu_2S}$ ($\gamma_{Cu_2S} > 1$), then $\gamma_{Cu_2S} > \gamma_{Ag_2S}$ and $\rho_{Cu_2S} > 1$. A full mathematical derivation of the Wagner-Allanore reference state as well as a demonstration of its utility in electrochemical analysis is given in [22].

As this approach is focused on cathode chemistries and their relation to the electrolyte, the study herein focuses on the simplest case of selectively electrowinning

Ag and Cu from their respective sulfides, with an inert graphite anode. Thus, there are two competing reduction reactions at the cathode:

$$\mathrm{Ag}^{+} + e \rightarrow \mathrm{Ag} \tag{6}$$

$$\mathrm{Cu}^{+} + e \rightarrow \mathrm{Cu} \tag{7}$$

and just one single oxidation reaction at the anode:

$$\mathrm{S}^{2-} \rightarrow \mathrm{S}_2 + 4e \tag{8}$$

In this paper, this approach is used for a methodical study of the relative thermodynamics of Ag_2S and Cu_2S in a BaS-La_2S_3 supporting electrolyte. This is carried out via equilibration experiments with a Cu metal reference and differing concentrations of Ag_2S and Cu_2S. The results of this equilibration study are evaluated with EESD's to predict which concentrations favor electrochemical separation and which concentrations favor co-deposition. A series of electro-winning experiments to test this model are presented and used for further evaluation of the sulfides' thermodynamics. The comparative discussion of findings from two studies further evaluates the role of non-standard state thermodynamics, the possible utility of the modeling method for investigation of unknown electrolytes, and the feasibility of sulfide-based Ag-Cu separation.

2. Experimental Methods

2.1. Sample Preparation

Barium sulfide (BaS, Alfa Aesar, 99.7% metals basis), lanthanum sulfide (La_2S_3, Strem Chemicals, 99.9% metals basis), copper sulfide (Cu_2S, Strem Chemicals, 99.5% metals basis), and silver sulfide (Ag_2S, Alfa Aesar, 99.9% metals basis) were used to prepare the electrolyte. The BaS-La_2S_3 supporting electrolyte was fixed at 90wt% of the total electrolyte. The remaining 10% consisted of Cu_2S-Ag_2S.

It was observed that a homogenous sulfide melt could not be obtained if BaS, La_2S_3, Cu_2S, and Ag_2S were mixed as powders in a crucible and melted together at high temperature. However, BaS, La_2S_3, and Cu_2S could be melted easily. Therefore, a two-step melting process was devised. A large batch of 90% BaS-La_2S_3, 10% Cu_2S "master mix" was first melted at 1523 K in an argon atmosphere (Ar, Airgas, Ultra High Purity). The resulting sulfide was then crushed back into powder form in an argon glovebox (Ar, Airgas, Ultra High Purity), and the necessary amount of Ag_2S to reach the desired final concentration was measured. Additional amounts of BaS-La_2S_3 were also added in order to maintain the supporting electrolyte at 90%. This new mix was then melted a second time in argon atmosphere. Thus, all electrolytes tested herein had an electroactive content of 10% (Ag_2S and Cu_2S).

For all melts, the sulfides were contained in a crucible machined from graphite (C, The Graphite Store, Grade EC-16) and fitted with a graphite cap that fit tightly into the crucible in order to limit possible sulfide volatilization. The experimental setup is shown in Figure 3. The graphite crucible was loaded into an alumina tube and placed into a vertical tube furnace (Lindberg/Blue M^{TM} Mini-Mite^{TM}). Inside the tube, an alumina rod containing either a sheathed “Type R" or “Type C" thermocouple served as a stage to both measure the temperature of the crucible as well as hold the crucible in the furnace hot zone.

2.2. Activity Measurements

Pure silver (Ag, Alfa Aesar, 99.999% metals basis) was used as the metal for equilibration experiments to measure relative activity. Silver containing small quantities of oxygen is known to violently expel oxygen upon solidification, and with it, small amounts of silver [26]. This phenomenon was observed to occur in silver samples during sulfide equilibration, hindering efforts to fully analyze the metal post-equilibrium. Therefore, the silver was de-oxygenated prior to experimentation. Approximately 0.1 g of Ag was melted in an arc melter (Compact Arc Melter MAM-1, Edmund Buhler) under Ar atmosphere in the presence of a zirconium oxygen getter (Zr, Alfa Aesar, 99.5% metals basis (excluding Hf), Hf 3%).

The de-oxygenated silver was then combined with the pre-melted sulfide in a graphite crucible and after evacuating and purging with Ar three times, was allowed to equilibrate at 1523K for 24 hours. At this time, the sample was lowered from the hot zone into the cooling zone (Figure 3). As the cooling zone was near the Ar inlet, the flow of Ar was increased to allow for an even more rapid cool. Once fully cool, the metal was mounted in epoxy, polished, and examined by scanning electron microscopy energy dispersive X-ray spectroscopy (SEM-EDS) to determine the Cu-Ag ratio. The sulfide was analyzed by an inductively coupled plasma atomic emission spectrometer (ICP-AES) in order to measure the change in content of Ba, La, S, Cu, and Ag.

2.3. Electrochemistry

A schematic of the electrochemical cell used for all experiments is shown in Figure 4. A two-electrode setup was used for the electrolysis experiments, with a liquid metal cathode consisting of either Ag or a Ag-Cu alloy (Ag, Alfa Aesar, 99.9985% metals basis), (Cu, Alfa Aesar, 99.999% metals basis), and a graphite anode (C, Alfa Aesar, 99.9995% metals basis). 5g of a BaS-La_2S_3-Cu_2S-Ag_2S electrolyte was prepared using both the materials and the two-step pre-melting process described above. The Ag-Cu alloy was prepared by melting approximately 5g of metal inside the arc melter 3 times, flipping the solidified metal piece in between melts in order to ensure homogeneity.

Both the metal and sulfide were then loaded into a graphite crucible with its sides sheathed by an alumina tube. A molybdenum wire (Mo, Ed Fagan Inc., ASTM B387 Type 361, 99.95% pure) was threaded into the bottom of the graphite crucible and secured with graphite paste (PELCO High Temperature Carbon Paste, Ted Pella, Inc.) to provide electrical contact to the cathode. This Mo wire was protected by an alumina tube that provided mechanical support to the setup and also contained a type C thermocouple used to monitor the cell's temperature.

A second Mo rod was threaded into the graphite anode, which, after being secured with graphite paste, was positioned just above the electrolyte, and the entire setup was loaded into a vertical tube furnace (Lindberg/Blue M^{TM} $\mathrm{Mini\text{-}Mite}^{\mathrm{TM}}$) and heated to 1523 K after being evacuated and purged with argon (Ar, Airgas, Ultra High Purity) three times. The Ag or Ag-Cu cathode had a diameter of 1.25 cm, while the C anode had a diameter of 0.305 cm.

Once the electrolyte was fully molten, the anode was lowered into the melt and galvanostatic electrolysis was run immediately to minimize any equilibrium exchange. At the end of the experiment, the electrochemical cell was immediately quenched by lowering the crucible out of the hot zone, the center of the furnace where the heat is concentrated, to the bottom of the furnace tube where cold Ar flows in. As in the quench methodology described above, the flow of Ar into the tube was increased in order to facilitate a more rapid quench.

Electrolysis experiments were run using a Gamry Potentiostat/Galvanostat (Gamry Instruments, Reference 3000), and temperature was monitored using an Omega data aquisition system (Omega Engineering, Model QMB-DAQ-55). All electrolysis experiments were run at a low cathode current density to minimize kinetic effects: $12mA/cm^2$.

Post-experiment, the metal cathode was separated from the sulfide electrolyte and was mounted in epoxy, polished, and examined using a scanning electron microscope's energy dispersive X-ray spectroscopy (SEM-EDS) to measure compositional changes from the initial Cu-Ag alloy.

3. Results

3.1. Activity Measurements

Upon examining the equilibrated metal, it was found that some exchange had taken place between Ag and Cu. Figure 5a shows the amounts of Cu measured in the Ag metal post-experiment. Cu content varied from as low as 0.03 to 0.21 (molar fraction). Generally, as the concentration of Cu_2S increased along the Ag_2S-Cu_2S pseudobinary, the more Cu was found in the metal. However, when $\frac{x_{\mathrm{Cu_2S}}}{x_{\mathrm{Cu_2S}}+x_{\mathrm{Ag_2S}}} = 0.4$, there was a notable increase of Cu concentration in Ag metal.

The Ag-Cu equilibrium electrochemical synthesis diagram from Figure 2 was used to determine the equilibrium difference in reduction potentials of Ag_2S and Cu_2S. This potential difference was used to compute the relative activity a_{Cu_2S}. Figure 5b shows the Wagner-Allanore activity coefficient ρ_{Cu_2S} as a function of Cu_2S concentration.

On the Cu_2S-rich half of the Ag_2S-Cu_2S pseudobinary, $\rho_{Cu_2S} \approx 1$. This indicates that Ag_2S and Cu_2S are behaving ideally with respect to one another in the BaS-La_2S_3 supporting electrolyte. Although the absolute activities of Ag_2S and Cu_2S are still unknown, this result means that both species interact with the supporting electrolyte in a similar way: if the absolute activity of Ag_2S is found to deviate positively from ideality, then Cu_2S will also deviate positively by approximately the same amount.

ρ_{Cu_2S} begins to increase on the Ag_2S-rich half of the pseudobinary. At $\frac{x_{\mathrm{Cu_2S}}}{x_{\mathrm{Cu_2S}}+x_{\mathrm{Ag_2S}}} = 0.4$, there is a sharp increase in ρ_{Cu_2S}, before decreasing as Ag_2S content continues to increase. However, ρ_{Cu_2S} does not approach 1, as it did in the Cu_2S-rich region. Instead, when Cu_2S content is less than 0.2, ρ_{Cu_2S} starts to increase again with Ag_2S content. At very low concentrations of Cu_2S, $\rho_{Cu_2S} \approx 14$. Table A1 summarizes the experimental results of equilibration across the entire pseudobinary, and Figure A1 shows the variation of the natural logarithm of the Wagner-Allanore activity coefficient, $\ln \rho_{Cu_2S}$ as a function of Cu_2S concentration.

In order to understand why ρ_{Cu_2S} increased suddenly at $\frac{x_{\mathrm{Cu_2S}}}{x_{\mathrm{Cu_2S}}+x_{\mathrm{Ag_2S}}} = 0.4$, further experimentation was necessary. A mix of BaS-La_2S-Cu_2S-Ag_2S electrolyte whose electroactive portion contained relative fractions of 0.4 Cu_2S and 0.6 Ag_2S was melted in a narrow, thin, cylindrical graphite crucible and allowed to equilibrate for 24 hours. At this time, the crucible was dropped from the furnace hot zone into a small pool of liquid gallium for a more aggressive quench. The sample was then removed from the crucible and sectioned lengthwise before being analyzed by SEM-EDS.

As shown in Figure 6, upon solidification, two main phases were observed to form: a primary phase, and a secondary intergrain phase. Examination of each phase under SEM-EDS showed a similar segregation of Ag and Cu between the two phases as that observed when looking at the overall segregation of Cu and Ag as a function of height in the crucible. The Ag-Cu content in the first phase to form, the primary phase, contained 0.65 Ag on average, while the secondary phase contained only 0.52. In certain areas of the crucible, a tertiary phase was occasionally observed to form. There was no significant Cu-Ag segregation observed in this phase.

Figures 7a and 7b show the variation in Cu and Ag content in the electrolyte as a function of height inside the crucible. Figure 7a shows that there was a higher concentration of Ag sulfides at the bottom of the crucible, while the electrolyte near the top was enriched in Cu sulfide. The average Ag-Cu content in the bottom half of the crucible was 0.66 Ag, while the average Ag-Cu content in the top half of the crucible was only 0.57 Ag. The average overall Ag-Cu content was 0.62 Ag.

3.2. Electrochemistry

Figure 8 shows the total cell voltage measured during a series of $12mA/cm^2$ galvanostatic experiments in a BaS-La_2S_3-Cu_2S-Ag_2S electrolyte containing 10% (Cu_2S + Ag_2S). The electroactive (non-supporting) portion of this electrolyte was chosen to contain $0.5Cu_2S$-$0.5Ag_2S$, as the activity study revealed Cu_2S as Ag_2S behave ideally with respect to one another at this concentration. Additionally, production of Ag during electrolysis would

Table 1: Cu content in cathode measured before and after electrolysis at $12 mA/cm^2$.

initial Cu	0	0	0.045	0.06	0.1
final Cu	0.008	0.0114	0.04	.053	0.073
Δ Cu	0.008	0.0114	-0.005	-0.007	-0.027
electrolysis duration (hr)	1	3.5	1	1	1

deplete the electrolyte further in Ag_2S, keeping the molten sulfide in an ideal regime while avoiding the complex phase relations noted to occur at $0.6Ag_2S$-$0.4Cu_2S$.

In order to investigate possible refining effects, the starting cathode composition contained varying amounts of Cu, from 0 to 0.1 mole fraction. The measured cell voltage gradually increased in magnitude over the time of the experiment, rather than stabilizing around one value. The electrochemical signals displayed regular oscillations, likely a result of heating element and thermocouple interference, but were overall very stable throughout electrolysis.

Table 1 shows the change in cathode composition after electrolysis, and Figure 9 compares the measured composition change to the equilibrium cathode Cu content. Depending on the starting cathode composition, either Ag or Cu was reduced from the electrolyte to the metal. It can be seen that when starting with a cathode of pure Ag, Cu is deposited on the cathode. When electrolysis was only run for 1 hour, the cathode was found to contain 0.008 Cu. However, when electrolysis was run for a longer amount of time, 3.5 hours, further enrichment of the cathode was observed: the final measured composition was 0.0114 Cu.

If the starting cathode composition contained Cu, the cathode was enriched in Ag instead. In these cases, the shift in cathode composition appeared to be proportional to how far the composition was from equilibrium (Figure 9). An Ag enrichment by a mole fraction of 0.027 was observed to take place when the starting alloy contained 0.1 Cu, while smaller shifts of 0.007 and 0.005 were found when the starting alloy contained 0.06 Cu and 0.045 Cu, respectively.

4. Discussion

4.1. Activity Measurements

Despite a 0.257 V decomposition potential difference between Ag_2S and Cu_2S, significant exchange between Cu_2S and Ag metal was observed to occur spontaneously, forming Cu metal and Ag_2S. The extent of this exchange was greatly influenced by the electrolyte composition, in particular by the relative amounts of Ag_2S and Cu_2S. On the Cu_2S-rich side, $\rho_{Cu_2S} \approx 1$ and the observed Cu content in the metal was consistent with ideal-solution predictions from the electrochemical synthesis diagrams. When Ag_2S and

Cu_2S behave ideally relative to one another, they are interacting with the supporting electrolyte in a similar way and the electrolyte thermodynamics do not contribute to co-deposition. This result indicates that, when the electrolyte is rich in Cu_2S, the observed alloying of Ag and Cu comes from the thermodynamic drive for mixing the two metals.

In contrast, when the electrolyte contains more Ag_2S, the electrolyte begins to deviate from ideality. More Cu is alloyed into the Ag than would be predicted from an EESD using an ideal-solution assumption. The activity coefficient ρ_{Cu_2S} was found to deviate positively from ideality in this concentration range. Additionally, there was a sharp increase in the activity coefficient when the $\frac{x_{\mathrm{Cu_2S}}}{x_{\mathrm{Cu_2S}}+x_{\mathrm{Ag_2S}}} = 0.4$. This corresponded to a larger amount of Cu alloying in the Ag metal.

$\rho_{Cu_2S} > 1$ signifies that Cu_2S has a higher activity coefficient in the electrolyte than Ag_2S. Relative to Ag_2S, Cu_2S has a more positive deviation from ideality. A positive deviation from ideality signifies an increase in Gibbs energy upon mixing, or a relative repulsion between phases in the electrolyte, while a negative deviation from ideality signifies an increased energetic drive for mixing. Therefore, $\rho_{Cu_2S} > 1$ indicates that the BaS-La_2S_3 electrolyte favors energetic bonds with Ag_2S over Cu_2S. Such behavior is supported by the observation that a BaS-La_2S_3-Ag_2S electrolyte required a higher temperature to melt.

The sudden increase in ρ_{Cu_2S} at $\frac{x_{\mathrm{Cu_2S}}}{x_{\mathrm{Cu_2S}}+x_{\mathrm{Ag_2S}}} = 0.4$ suggests similar preference for bonds between Ag_2S and the supporting BaS-La_2S_3 electrolyte at this composition. One possible explanation for this phenomenon could be the formation of a compound near this composition. This would result in short-range ordering between Ag_2S and the BaS-La_2S_3 supporting electrolyte in the liquid after this compound melted. Since ρ_{Cu_2S} is a relative value, however, it only signifies that there is a strong preference for the supporting electrolyte to interact with Ag_2S instead of Cu_2S. Therefore, while short-range ordering between Ag_2S and the supporting electrolyte is possible, it is also possible that there is phase separation between Cu_2S and the rest of the supporting electrolyte.

4.2. Gallium Quench Experiment

During the gallium quenching experiment, it was found that there was an increased concentration of Ag_2S towards the bottom of the crucible, while the top of the crucible was richer in Cu_2S (Figure 7a). Furthermore, while the overall concentration of the sulfide remained near the original concentration, the ratio of $\frac{x_{\mathrm{Cu_2S}}}{x_{\mathrm{Cu_2S}}+x_{\mathrm{Ag_2S}}}$ in the bottom half of the crucible differed by 0.1 from the top half. This result points to evidence of possible phase separation between Cu_2S-rich electrolyte and Ag_2S-rich electrolyte in the liquid phase, with the denser Ag_2S-rich liquid sinking to the bottom of the crucible.

Additionally, the first two phases to nucleate upon solidification also displayed similar segregation of Cu_2S and Ag_2S (Figure 7b). The primary phase was Ag_2S-rich, with an average composition near that of the average composition of the Ag_2S-rich bottom half of the crucible. That the Ag_2S-rich phase was the first to nucleate supports the hypothesis that there is favorable bonding between Ag_2S and the supporting electrolyte, and is consistent with observations of higher melting points for Ag_2S-rich electrolytes. The second phase to form contained higher amounts of Cu_2S, similar to the top half of the crucible.

The results for both micro- and macro- scale segregation suggest there are very different energetic interactions between Ag_2S and the supporting electrolyte, and between Cu_2S and the supporting electrolyte. These results are also consistent with increase in ρ_{Cu_2S} at this concentration. Although ρ_{Cu_2S} is a relative activity, it retains important information about electrolyte interactions. Deviations from ideality that suggest certain phase phenomena, such as phase separation or compound formation, are still measured. In the case of a BaS-La_2S-Cu_2S-Ag_2S electrolyte, these phenomena could be confirmed by microscopy (Figure 6), which revealed that Ag_2S and Cu_2S interact differently with BaS-La_2S.

4.3. Electrolysis

It can be seen that when starting with a cathode of pure Ag, there is a strong drive for Cu deposition in order to reach this equilibrium composition. This drive causes preferential reduction of Cu instead of Ag, even though the measured difference in reduction potential between Cu_2S and Ag_2S for this electrolyte composition should be 265mV, with Ag being the more cathodic, or noble, species. In order to affirm that Cu deposition was an electrochemical phenomena, the dependence of concentration shift on electrolysis time was measured. It was found that the longer an experiment was run, the more Cu was alloyed into the cathode (Figure 9).

When the cathode contains 0.1 Cu, both the electrolyte and the cathode favor Ag deposition. With an equilibrium concentration of 0.058 Cu, increasing Ag content through deposition will lower the Cu concentration of the cathode and thus lower its Gibbs energy. When the cathode contained moderate amounts of Cu, such as 0.045 or 0.06, the cathode was closer to its equilibrium composition and there was less of a drive for Ag deposition as a result. The cathode was observed to increase in Ag content through both experiments.

When the cathode contained 0.045 Cu, one might expect that Cu be deposited on the cathode instead of Ag in order to reach the equilibrium concentration. However, Ag was deposited instead. There are several reasons why this may occur. First, it has been shown that the kinetic and transport effects at play during electrolysis cannot be neglected entirely when using an equilibrium electrochemical synthesis diagram to analyze electrochemical data [22]. It is also possible that local concentration variations in the vicinity of the cathode caused the equilibrium concentration to shift, favoring Ag deposition instead. In order to allow for the anode to be lowered into the melt right at the start of electrolysis, the electrochemical cell was open at the top. The absence of a cap may have allowed for certain elements to volatilize during the experiment, which could also shift the electrolyte concentration and in turn effect the equilibrium

Cu concentration in the cathode.

4.4. Perspectives on Synthesis Diagrams and Thermodynamic Modeling

The results of this Cu_2S and Ag_2S study give an important insight into the role of equilibrium electrochemical synthesis diagrams on thermodynamic modeling and experiment prediction. The ability to integrate the mixing chemistry of the metallic species with electrochemical behavior allows for more accurate prediction of the reduced species than can not be gained by standard-state analysis alone. When the composition of the cathode after equilibration is measured experimentally, the thermodynamic properties of the electrolyte can be indirectly measured. Since this method lacks a true thermodynamic reference, it is not possible to measure the activities of the supporting electrolytes independently. However, the ratio of activities of the electroactive species can be measured, and this data can be used to gain further important insights on the electrochemical system.

As shown above, this approach, while unorthodox, allowed for a rapid analysis of the BaS-La_2S_3-Cu_2S-Ag_2S electrolyte. Figures 5 and 7 demonstrate how relative activity can indicate true thermodynamic phenomena, without the need for a full-scale activity study. In systems like molten sulfides, where finding a stable thermodynamic reference is challenging, this method is particularly attractive. Additionally, Figure 9 applies the thermodynamic information gained from the relative activity study to electrochemical behavior during electrolysis. Although further work is necessary to understand the non-equilibrium effects, the agreement between the thermodynamic predictions and the observed results are very promising.

It is hypothesized that this method of precious metal refining can be expanded beyond Ag to Au and PGM. In preliminary experiments, gold showed promising solubility in molten sulfide media [18]. Given the demonstrated ability of BaS-La_2S_2-Cu_2S to act as a supporting electrolyte, this system should be a first choice for future research in this direction. However, the interactions between gold, platinum, or iridium sulfides and the electrolyte are not known. It is possible these interactions will not support separation, and the electrolyte composition will need to be revisited. In such case, the modeling approach demonstrated above would prove useful for a quick screen of optimal electrolyte systems.

5. Conclusions

The unique solubility properties of molten sulfides suggest that they may be used to develop an alternative, streamlined method of processing precious metals such as Ag from Cu-rich sources. Through relative activity measurements of a BaS-La_2S_2-Cu_2S-Ag_2S electrolyte containing 10% Cu_2S-Ag_2S, it was found that Cu_2S and Ag_2S behaved ideally with respect to one another when the electrolyte was richer in Cu_2S, and started to deviate from ideality, with an energetic penalty to mixing, when the electrolyte was richer in Ag_2S. In particular, there was a large positive deviation from ideality when $\frac{x_{\mathrm{Cu_2S}}}{x_{\mathrm{Cu_2S}}+x_{\mathrm{Ag_2S}}} = 0.4$. This result suggested a strong tendency away from mixing Cu_2S and Ag_2S, which was later confirmed with aggressive quench experiments.

Electrolysis experiments showed that at low current densities, the thermodynamics of the BaS-La_2S_2-Cu_2S-Ag_2S electrolyte influenced the final composition of the cathode. It was found that the cathode composition tended to approach the previously measured equilibrium concentration, enriching either in Cu or in Ag during electrolysis, when the starting cathode composition was far from the equilibrium point. When the starting cathode composition was closer to the equilibrium point, the cathode was consistently enriched in Ag, suggesting contribution of other phenomena. Further experimentation should be done in order to understand these contributions, including study of Cu and Ag deposition at various current densities and with other ratios of Cu_2S-Ag_2S. Additionally, it is recommended that future endeavors focus on electrorefining from a Cu-Ag alloy, in order to understand the effect anode chemistries can have on system efficacy.

The experiments and results demonstrated highlight the utility of a relative activity framework. When an electrolyte is particularly reactive and traditional activity measurements are challenging, or when fast screening of possible electrolytes for a new technology is desired, relative activity alongside equilibrium electrochemical synthesis diagrams can be used to predict electrorefining behavior from minimal information on cathode and electrolyte chemistry. This information is valuable to the electrochemist looking to design new processes or optimize old ones.

6. Acknowledgements

This work is the result of projects partially funded by the US DOE-AMO-EERE Office (DE-EE0008316) and the US National Science Foundation (ID 1760025)

7. References

[1] Ailiang Chen, Zhiwei Peng, Jiann-Yang Hwang, Yutian Ma, Xuheng Liu, and Xingyu Chen. Recovery of silver and gold from copper anode slimes. *JOM Journal of the Minerals, Metals and Materials Society*, 67:493–502, 2015.

[2] J. D. Scott. Electrometallurgy of copper refinery anode slimes. *Metallurgical Transactions B*, 21:629–635, 8 1990.

[3] T.T. Chen and J.E. Dutrizac. Mineralogical characterization of a copper anode and the anode slimes from the la caridad copper refinery of mexicana de cobre. *Metallurgical and Materials Transactions B*, 36B:229–240, 2005.

[4] D R Swinbourne, G G Barbante, and A Sheeran. Tellurium distribution in copper anode slimes smelting. *Metallurgical and Materials Transactions B*, 29:555–562, 1998.

[5] S Beauchemin, T T Chen, and J E Dutrizac. Behavior of antimony and bismuth in copper electrorefining circuits. *Canadian Metallurgical Quarterly*, 47:9–26, 2008.

[6] E.N. Petkova. Microscopic examination of copper electrorefining slimes. *Hydrometallurgy*, 24:351–359, 1990.

[7] S.A. Mastyugin and S.S. Naboichenko. Processing of copper-electrolyte slimes: evolution of technology. *Russian Journal of Non-Ferrous Metals*, 53:367–374, 2012.

[8] J Hait, R K Jana, and S K Sanyal. Processing of copper electrorefining anode slime: a review. *Trans. Inst. Min. Metall. C.*, 118:240–252, 2009.

[9] T.T. Chen and J.E. Dutrizac. Mineralogical overview of the behavior of gold in conventional copper electrorefinery anode slimes processing circuits. *Mining, Metallurgy & Exploration*, 25:156–164, 2008.

[10] C Segawa and T Kusakabe. Current operations in smm's slime treatment. 1996.

[11] Samira Sokhanvaran, Sang-Kwon Lee, Guillaume Lambotte, and Antoine Allanore. Electrochemistry of molten sulfides: Copper extraction from bas-cu2s. *Journal of the Electrochemical Society*, 163:D115–D120, 2016.

[12] Sulata K. Sahu, Brian Chmielowiec, and Antoine Allanore. Electrolytic extraction of copper, molybdenum and rhenium from molten sulfide electrolyte. *Electrochimica Acta*, 243:382–389, 2017.

[13] *Precious Materials Handbook*. Umicore AG & Co, KG, 1 edition, 2012.

[14] G.A. Pal'yanova and N.E. Savva. Some sulfides of gold and silver: composition, mineral mineral assemblage, and conditions of formation. *Theoretical Foundations of Chemical Engineering*, 42:749–761, 2008.

[15] Galina Palyanova, Nick Karmanov, and Natalie Savva. Sulfidation of native gold. *American Mineralogist*, 99:1095–1103, 2014.

[16] Mark D. Barton. The ag-au-s system. *Economic Geology*, 75:303–316, 1980.

[17] K G Fisher. Refining of gold at the rand refinery, 1987.

[18] Mary-Elizabeth Wagner. New methodology to model metal chemistry at high temperature, 6 2021.

[19] A. N. Baraboshkin. Electrocrystallization from molten salts. *Moscow: Nauka*, 1976.

[20] V V Malyshev, H B Kushkhov, and V I Shapoval. High-temperature electrochemical synthesis of carbides, silicides and borides of vi-group metals in ionic melts. *Journal of Applied Electrochemistry*, 32:573–579, 2002.

[21] G. Kaptay. The conversion of phase diagrams of solid solution type into electrochemical synthesis

diagrams for binary metallic systems on inert cathodes. *Electrochimica Acta*, 60:401–409, 1 2012.

[22] Mary-Elizabeth Wagner and Antoine Allanore. Non-standard state thermodynamics of metal electrodeposition. *Electrochimica Acta*, 389, 9 2021.

[23] Caspar Stinn, Katsuhiro Nose, Toru Okabe, and Antoine Allanore. Experimentally determined phase diagram for the barium sulfide-copper(i) sulfide system above 873 k (600 °c). *Metallurgical and Materials Transactions B*, 48:2922–2929, 2017.

[24] Charles Cooper Rinzler. Quantitatively connecting the thermodynamic and electronic properties of molten systems, 2017.

[25] C H P Lupis. *Chemical Thermodynamics of Materials*. North-Holland, 1983.

[26] Manuel Eissler. *The Metallurgy of Silver: A Practical Treatise on the Amalgamation, Roasting and Lixiviation of Silver Ores Including the Assaying, Melting and Refining of Silver Bullion*. Crosby, Lockwood, and son, 3rd edition, 1896.

[27] C. W. Bale, E. Bélisle, P. Chartrand, S. A. Decterov, G. Eriksson, A. E. Gheribi, K. Hack, I. H. Jung, Y. B. Kang, J. Melançon, A. D. Pelton, S. Petersen, C. Robelin, J. Sangster, P. Spencer, and M. A. Van Ende. Factsage thermochemical software and databases, 2010-2016. *Calphad*, 54:35–53, 9 2016.

8. Figures

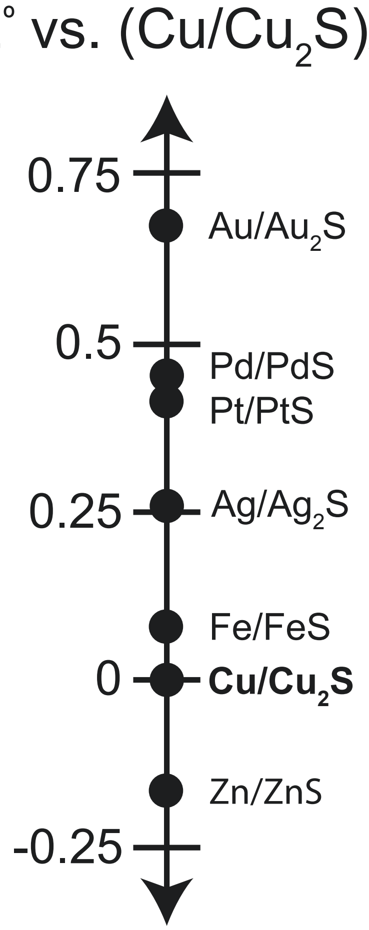

Figure 1: Standard-state electrochemical series for sulfides at 1523K, plotted vs. Cu/Cu_2S. The standard state of Cu_2S is defined as pure liquid Cu_2S at 1523K, 1 atm. reference [27, 16].

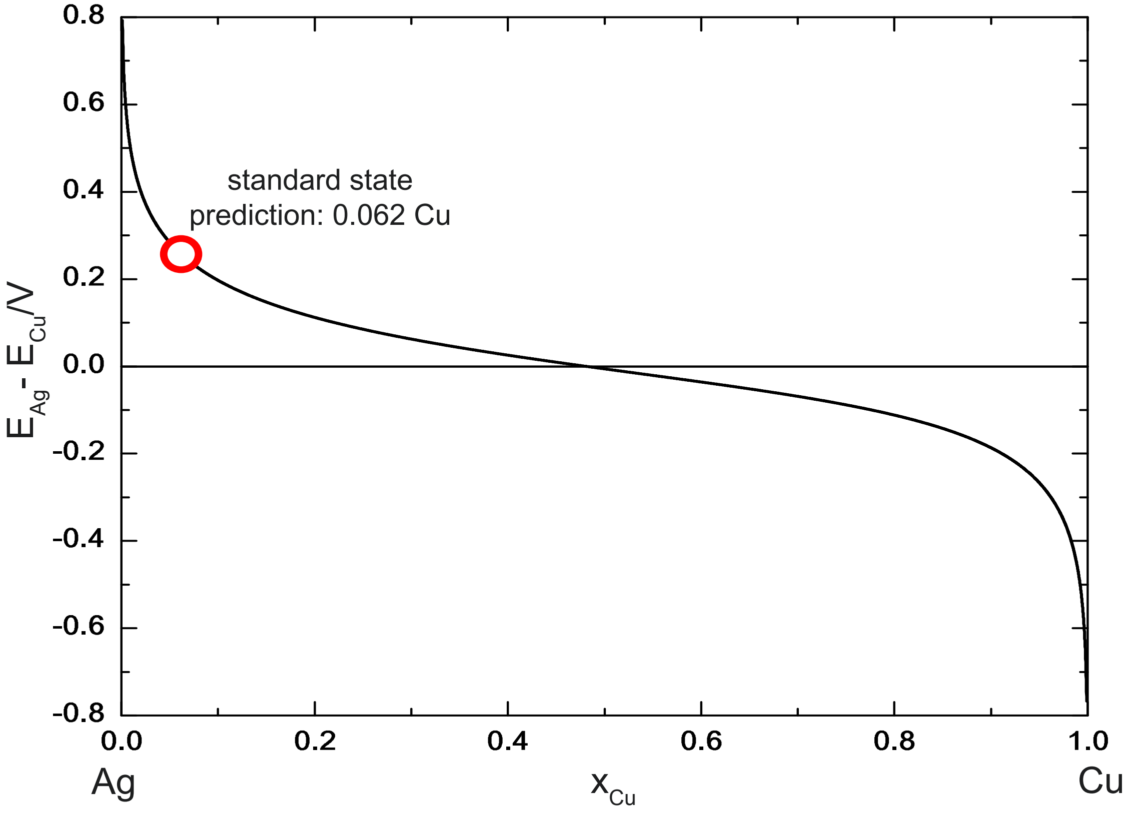

Figure 2: Electrochemical synthesis diagram for for the Ag − Cu/Ag_2S − Cu_2S system at 1523K with: ○: predicted concentration of Cu in Ag based on $E^{\circ}_{\mathrm{Ag}} - E^{\circ}_{\mathrm{Cu}} = 0.257$ V.

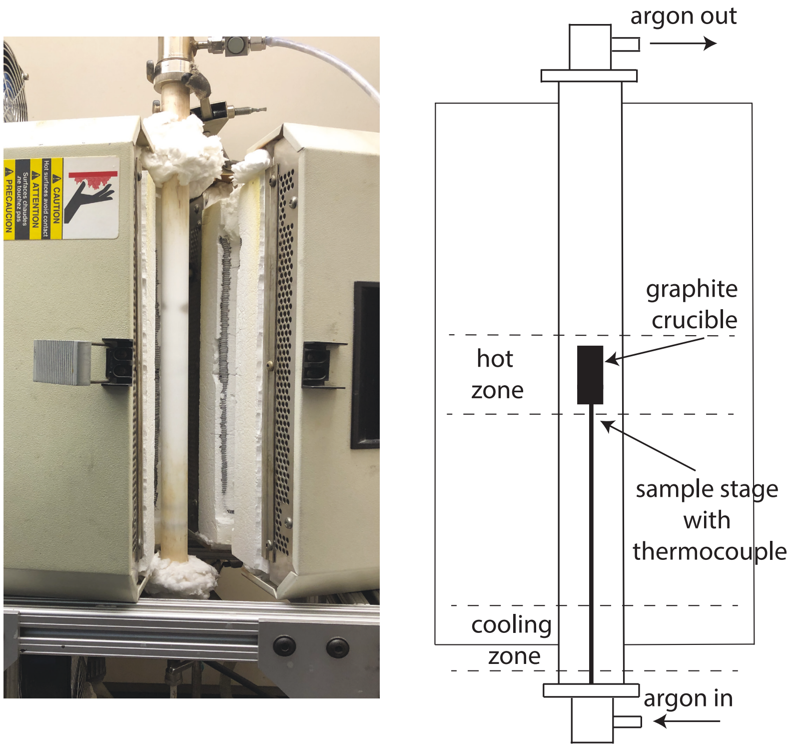

Figure 3: Left) furnace setup used for sulfide melts and equilibrium experiments. Right) schematic of setup showing hot zone and cooling zone.

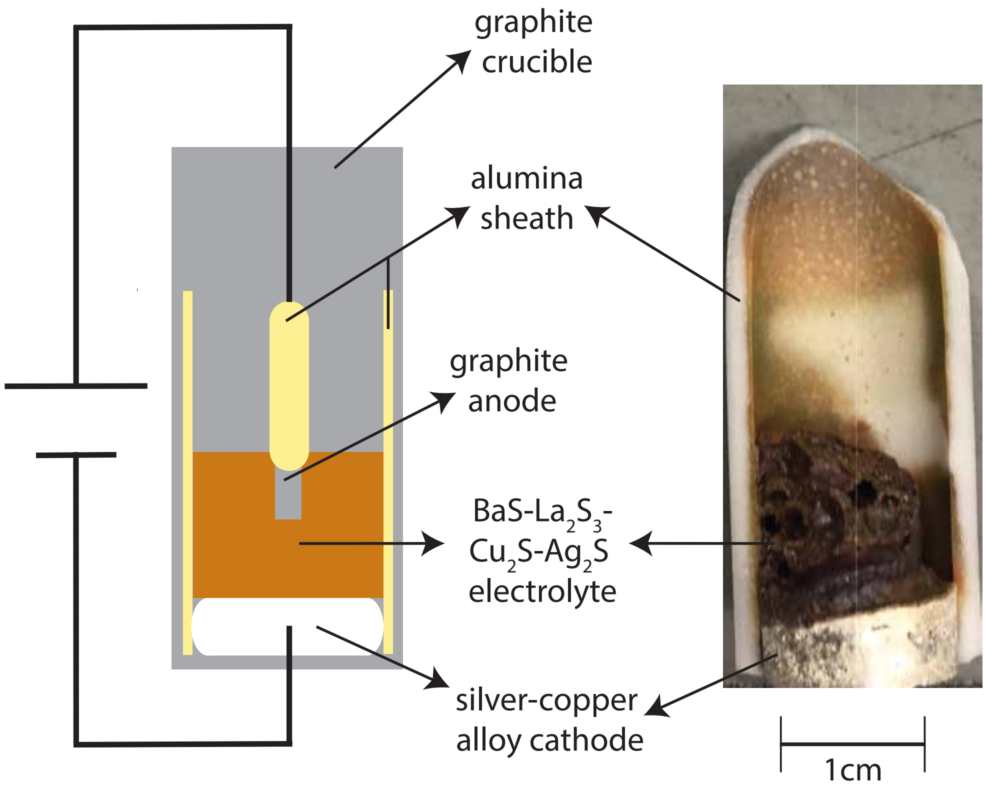

Figure 4: Left) schematic of electrochemical cell used for Cu-Ag electrolysis experiments. Right) cathode and electrolyte after electrolysis experiment

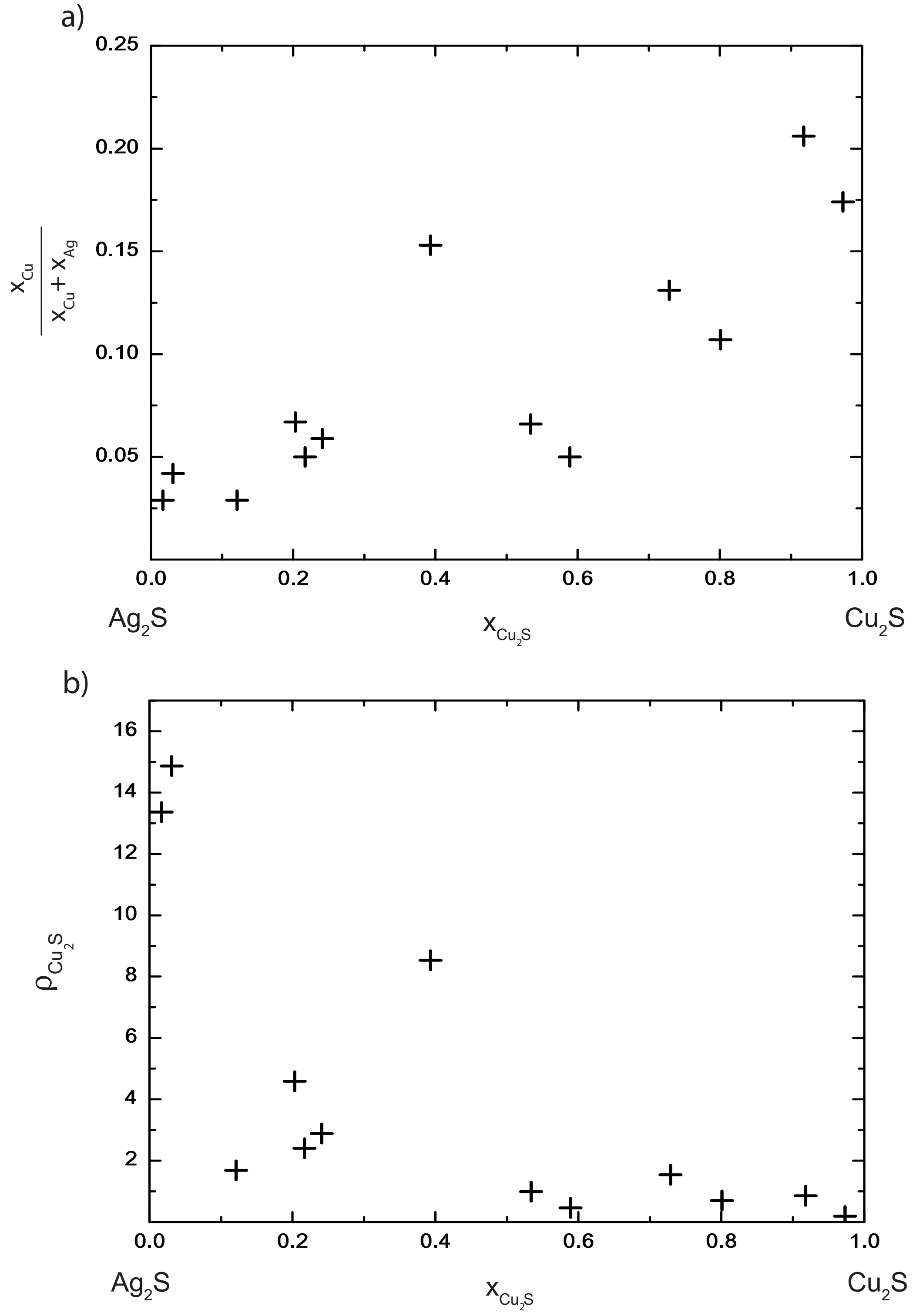

Figure 5: a) measured Cu content in Ag metal after equilibration with molten BaS-La_2S_3-Cu_2S-Ag_2S at 1523K for 24 hours. b) calculated relative activity coefficient ρ_{Cu_2S} in BaS-La_2S-Cu_2S-Ag_2S after equilibration with Ag metal at 1523K for 24 hours.

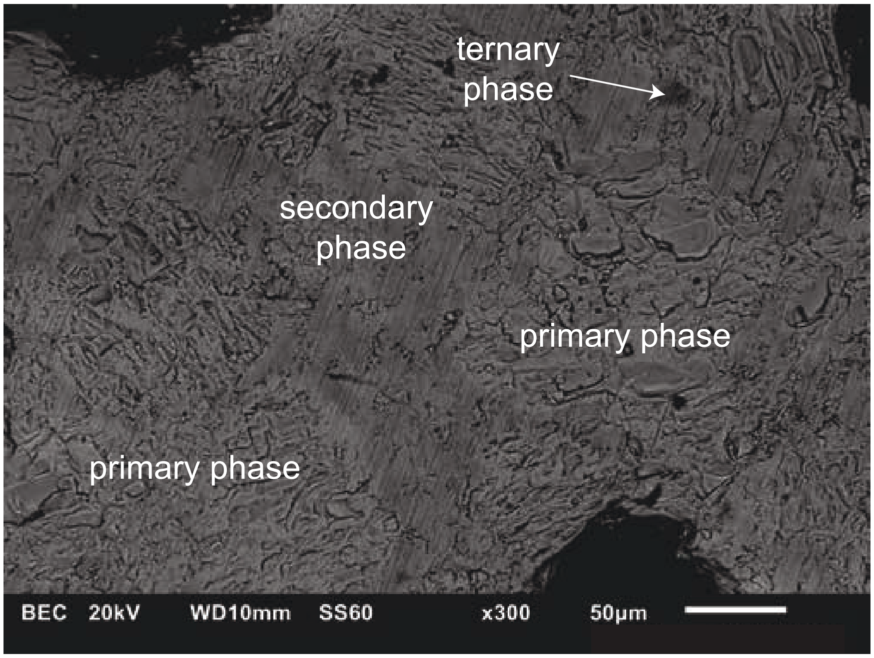

Figure 6: SEM image of typical microstructure of Ga-quenched BaS-La_2S-Cu_2S-Ag_2S electrolyte with an electroactive content of 0.4 Cu_2S and 0.6 Ag_2S. The "primary phase" had an average Ag content of 0.65 relative to Cu, while the "secondary phase" contained an average of 0.52. No significant segregation trend was observed in the tertiary phase.

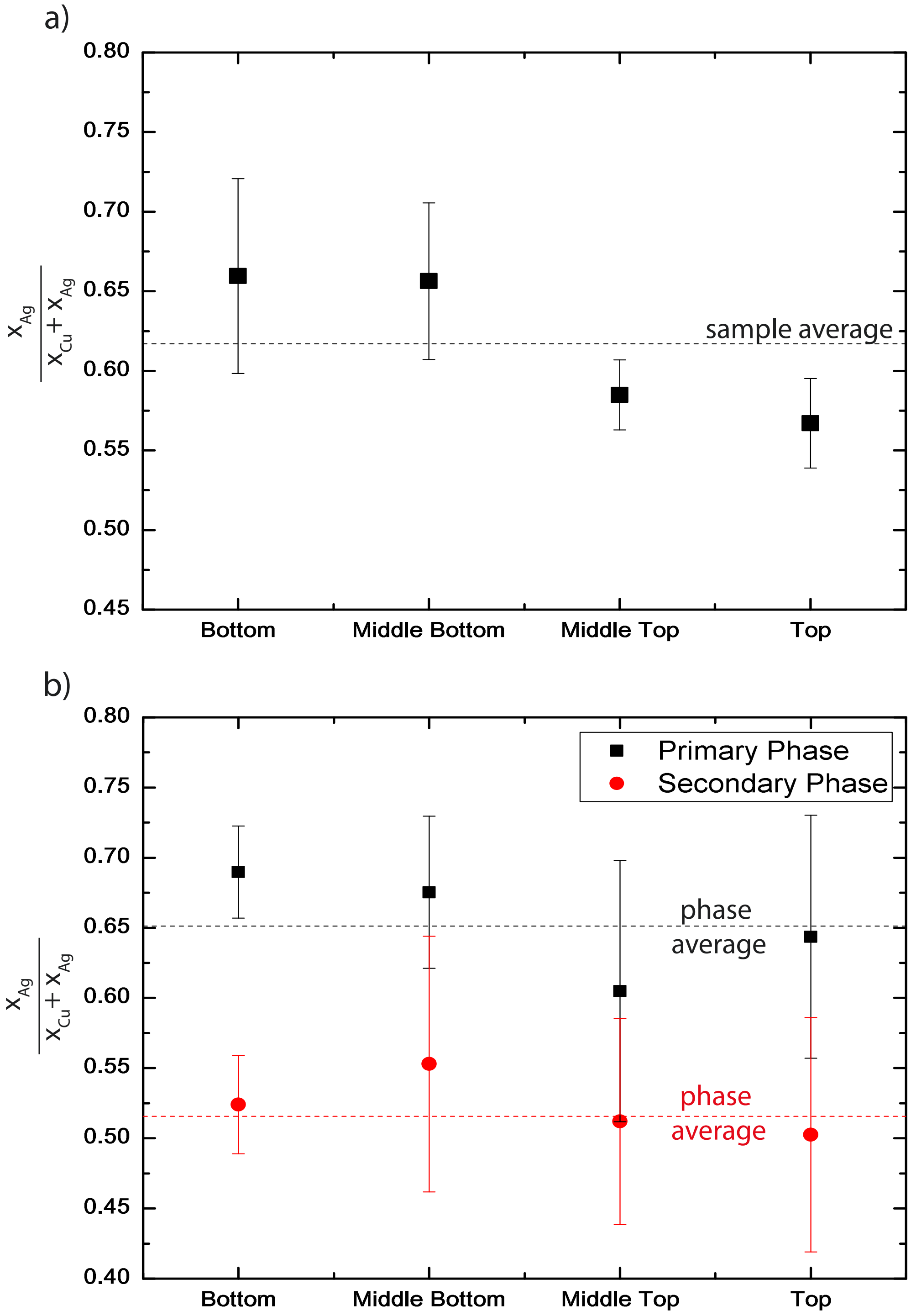

Figure 7: a) average $\frac{Ag}{Ag+Cu}$ ratio in a BaS-La_2S-Cu_2S-Ag_2S electrolyte with an electroactive content of 0.4 Cu_2S and 0.6 Ag_2S, as a function of height inside the crucible. b) measured Ag content relative to Cu in the primary and secondary phases of a BaS-La_2S-Cu_2S-Ag_2S electrolyte with an electroactive content of 0.4 Cu_2S and 0.6 Ag_2S, as a function of height inside the crucible.

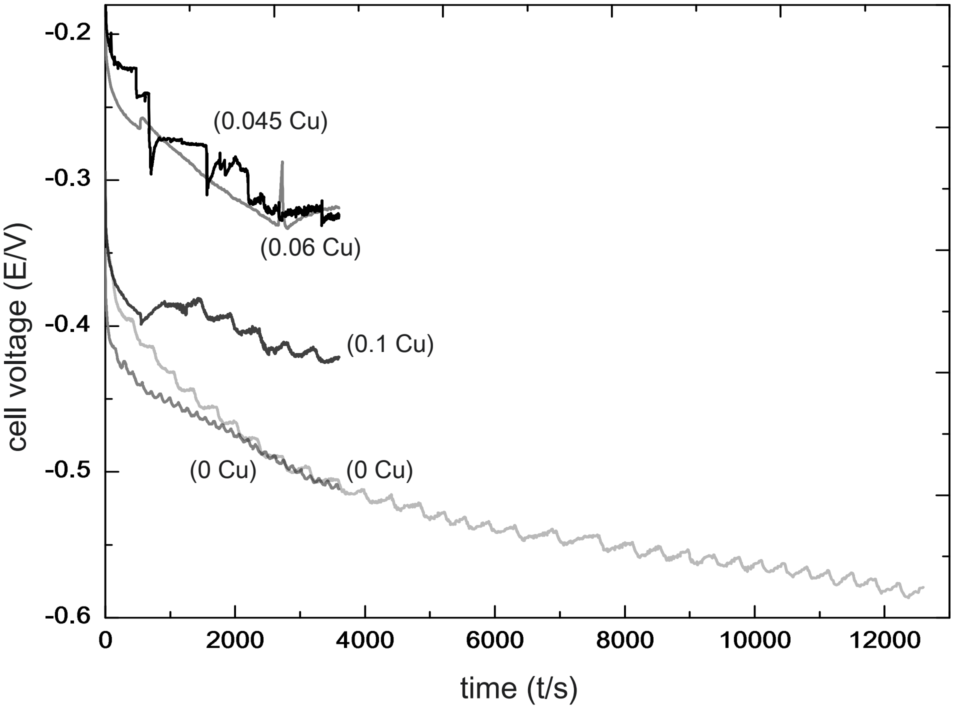

Figure 8: Galvanostatic measurements in a BaS-La_2S_3-Cu_2S-Ag_2S electrolyte for cathodes containing varying starting amounts of Cu in Ag (0 Cu, 0.045 Cu, 0.06 Cu, 0.1 Cu). Cathode current density: $12mA/cm^2$. Temperature: 1523 K.

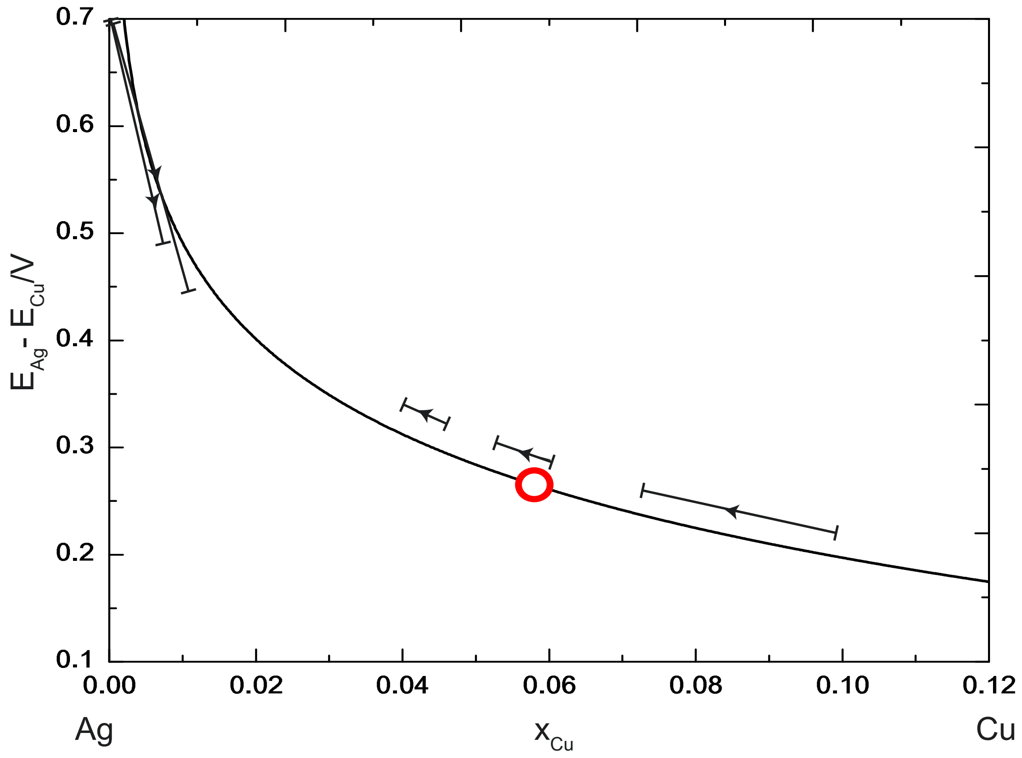

Figure 9: Equilibrium electrochemical synthesis diagram showing cathode compositions before and after electrolysis for a BaS-La_2S_3-Cu_2S-Ag_2S electrolyte containing equimolar proportions of Cu_2S and Ag_2S. ○: equilibrium Cu content in Ag cathode for this electrolyte in absence of electrolysis. →: direction of composition change during electrolysis

Appendix A.

Table A1: Cu content in Ag and measured ρ_{Cu_2S} after equilibration with Ag_2S and Cu_2S in a BaS-La_2S_3 supporting electrolyte.

$\frac{Cu_2S}{Cu_2S+Ag_2S}$	$\frac{Cu}{Cu+Ag}$	ρ_{Cu_2S}
0.02	2.9	13.4
0.03	4.2	14.9
0.12	2.9	1.7
0.203	6.7	4.6
0.217	5.0	2.4
0.241	5.9	2.9
0.393	15.3	8.53
0.534	6.6	0.9
0.589	5.0	0.5
0.729	13.1	1.5
0.801	10.7	0.7
0.918	20.6	0.9
0.973	17.4	0.2

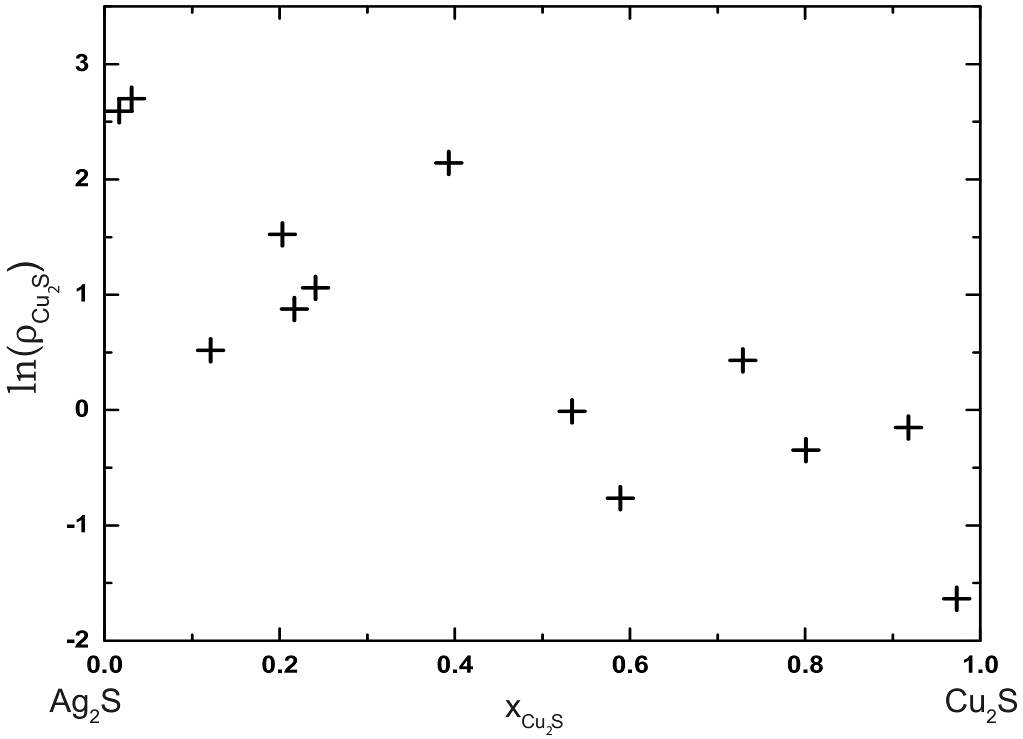

Figure A1: Natural logarithm of calculated activity coefficient $\ln \rho_{Cu_2S}$ in BaS-La_2S-Cu_2S-Ag_2S after equilibration with Ag metal at 1523K for 24 hours.